# Simulation on effect of poloidal power spectrum on lower hybrid wave propagation*

Qin Yong-Liang(秦永亮), Ding Bo-Jiang(丁伯江), Kuang Guang-Li(匡光力), Jia Hua(贾 华), and Zhang Li-Zhi(张立智)

*Institute of Plasma Physics, Chinese Academy of Sciences, Hefei* 230031, *China*

(Received 7 April 2009; revised manuscript received 8 September 2009)

The coupling of lower hybrid wave to the plasma is a crucial issue for efficient current drive in tokamaks. This paper establishes a new coupling model which assumes the antenna to be a curved face and the plasma to be a cylinder. Power spectrum considering the coupling between wave-guides in both poloidal and toroidal direction is simply estimated and discussed. The effect of the poloidal wave vector on wave propagation, power deposition and driven current is also investigated with the help of lower hybrid current drive code. Results show that the poloidal wave vector affects the ray tracing, and also has effect on power deposition and driven current. The effect of the poloidal wave vector on power deposition and driven current profile depends on plasma parameters. Preliminary studies suggest that it seems possible to control the current profile by adjusting the poloidal phase difference between the waveguide in poloidal direction.

**Keywords:** simulation, lower hybrid wave, poloidal wave vector, wave coupling

**PACC:** 5240, 5240D, 5240F, 5265

## 1. Introduction

Lower hybrid wave (LHW) is an efficient tool to drive one part of the current in tokamak to improve confinement by profile control and the lower hybrid current drive (LHCD) system has become a very important part of all present day experiments towards magnetically controlled fusion.

As we know, LHCD simulation including ray tracing, power deposition and driven current is very important to guide and analyse plasma experiments. Since power spectrum is a key input parameter determining the ray tracing and the power deposition, it is very essential to investigate the coupling between LHW and plasma. The previous model of LHW coupling to plasma was based on a 1-dimensional slab model firstly established by Brambilla in 1970s,[1] in which only the coupling between the toroidal waveguide's was considered and waveguides dimension in the poloidal direction was taken to be infinite. As a consequence, only the toroidal wave vector along the toroidal direction and the vertical wave vector along the radial direction are taken into account. In fact, the LHW antenna's dimension in the poloidal direction is not infinite and usually there are several rows in this direction. Also, due to the different distance between the antenna and the plasma in the different rows, some phase difference in the poloidal direction could exist. Considering such effects could lead to the poloidal wave vector in the poloidal direction. Similar work has been done by Berio S and Bilet Ph in 1996,[2] which considered it in the Cartesian coordinates with the step plus ramp model, whereas we treat it in the cylindrical coordinates with the ramp model. Also, effect of the poloidal wave vector on wave propagation has not been discussed there. If such a poloidal wave vector is considered, the direction of LHW launching into plasma will be changed. As a result, the LHW propagation in plasma, power deposition, and driven current could also be modified. Therefore, it is necessary to estimate the 2-dimensional power spectrum considering the coupling in both poloidal and toroidal directions, and to investigate the effect of the poloidal vector on ray tracing, power deposition and driven current.

In this paper, the calculation of spectrum considering the coupling in both directions will be briefly described in Section 2. In Section 3, some preliminary results are given and analysed, followed by a simple discussion in Section 4. Finally, a conclusion is given in Section 5.

*Project supported by the National Natural Science Foundation of China (Grant Nos. 10575104 and 10875149) and by Dean Foundation of Hefei Institute of Physical Science, Chinese Academy of Sciences.

© 2010 Chinese Physical Society and IOP Publishing Ltd

## 2. Description of mathematical calculation

Invoked from the calculation of toroidal spectrum[3] and also considering the poloidal dimension of the antenna, we can write the electric field and the magnetic field in the wave-guides as

$$E_I^{\rm wg}(\rho,\varphi,z) = \sum_{p=1}^{MJ}\theta_p(z)\sigma_p(y)\Bigg[\sum_{m=0}^{\infty}\sum_{n=0}^{\infty}(\alpha_{mnp}{\rm e}^{{\rm i}(k_{mn}\phi_1(I)+\phi_2(I)+\phi_3(I))} + \beta_{mnp}{\rm e}^{-{\rm i}(k_{mn}\phi_1(I)+\phi_2(I)+\phi_3(I))})\cos\frac{n\pi(z-z_p)}{b}\sin\frac{m\pi(y-y_p)}{a}\Bigg], \tag{1}$$

$$B_I^{\rm wg}(\rho,\varphi,z) = -{\rm i}\,k_0\sum_{p=1}^{MJ}\theta_p(z)\sigma_p(y)\Bigg[\sum_{m=0}^{\infty}\sum_{n=0}^{\infty}\frac{1}{{\rm i}\,k_{mn}}(\alpha_{mnp}{\rm e}^{{\rm i}(k_{mn}\phi_1(I)+\phi_2(I)+\phi_3(I))} - \beta_{mnp}{\rm e}^{-{\rm i}(k_{mn}\phi_1(I)+\phi_2(I)+\phi_3(I))})\cos\frac{n\pi(z-z_p)}{b}\Bigg)\sin\frac{m\pi(y-y_p)}{a}\Bigg]. \tag{2}$$

Here

$$\theta_p(z)=\begin{cases}1 & \text{for } z_p\le z\le z_p+b,\\ 0 & \text{otherwise,}\end{cases}$$

and

$$\sigma_p(y)=\begin{cases}1 & \text{for } y_p\le y\le y_p+a,\\ 0 & \text{otherwise,}\end{cases}$$

$$x_0=\rho\cos\varphi_0,\quad y_0=\rho\sin\varphi_0,$$
$$x=x_0-\rho\cos\varphi=\rho(\cos\varphi_0-\cos\varphi),$$
$$y=y_0-\rho\sin\varphi=\rho(\sin\varphi_0-\sin\varphi),$$

where $z$ is along the toroidal direction, $y$ is along the poloidal direction, and $x$ is along the vertical direction of wave-guides surface, $\rho$ and $\varphi_0$ are the radius and angle of antenna surface respectively. Other parameters are defined as follows: $z_p$ and $z_p+b$ are the edges of $p$-th wave-guide in $z$-direction, $y_p$ and $y_p+a$ are the edges of $p$-th wave-guide in $y$-direction, $m$ and $n$ are the $m$-th and the $n$-th propagating modes in the $p$-th wave-guide, $\alpha_{mnp}$ and $\beta_{mnp}$ are the amplitudes of incident wave and reflected wave, respectively, $\phi_1$ is poloidal phase difference of antenna, $\phi_2$ is the angle of different rows of antenna, $\phi_3$ is phase difference because of optical path difference LHW propagating in the antenna. $MJ$ is the number of waveguides, $I$ is the number of rows of antenna.

In the vacuum region, the electric field and the magnetic field can be written as

$$E_z^{\nu}(\rho,\phi,z)=\int_{-\infty}^{+\infty}\sigma(k_\parallel,k_y)({\rm e}^{{\rm i}\,k_\perp\rho\cos\phi}-y(k_\parallel,k_y){\rm e}^{-{\rm i}\,k_\perp\rho\cos\phi}){\rm e}^{{\rm i}\,k_\parallel z+{\rm i}\,k_y y}{\rm d}k_\parallel{\rm d}k_y, \tag{3}$$

$$B^{\nu}(\rho,\phi,z)=-k_0\int_{-\infty}^{+\infty}\sigma(k_\parallel,k_y)({\rm e}^{{\rm i}\,k_\perp\rho\cos\phi}+y(k_\parallel,k_y){\rm e}^{-{\rm i}\,k_\perp\rho\cos\phi}){\rm e}^{{\rm i}\,k_\parallel z+{\rm i}\,k_y y}{\rm d}k_\parallel{\rm d}k_y, \tag{4}$$

here $k_0$ is the wave vector in the vacuum, $k_\parallel$ and $k_y$ are the toroidal wave vector and the poloidal wave vector, respectively, $k_\perp$ is the vertical wave vector along the radial direction, $\sigma(k_\parallel,k_y)$ is the electric field of incident wave, $y(k_\parallel,k_y)$ is the reflection coefficient of electric field. The impedance in this area is

$$Z_\nu=\frac{{\rm i}\,E_z}{B}=-\frac{{\rm i}\,k_\perp}{k_0}\frac{1-y(k_\parallel,k_y){\rm e}^{-{\rm i}\,2k_\perp\rho\cos\phi}}{1+y(k_\parallel,k_y){\rm e}^{-{\rm i}\,2k_\perp\rho\cos\phi}}. \tag{5}$$

In the plasma region, as we know, the main feature determining the behaviour of the waves near the plasma edge is the cut-off which occurs where the local electron plasma frequency equals the applied frequency,[4] and typically, only the first few millimeters of the edge of plasma are important in determining coupling. The electric field and the magnetic field can be written as follows: when $n_\parallel<1$, or $k_\parallel<k_0$ (here, $n_\parallel$ is the toroidal refractive index), in the inner of plasma

$$E_z=C\left[{\rm J}_{1/3}(t_2\rho)\sin(\phi/3)+{\rm e}^{{\rm i}\,\pi/3}{\rm J}_{-1/3}(t_2\rho)\sin(-\phi/3)\right], \tag{6}$$

in the edge of plasma (only the first few millimeters of the plasma edge)

$$E_z = C\left[\mathrm{J}_{1/3}(t_1\rho)\sin(\phi/3) + \mathrm{J}_{-1/3}(t_1\rho)\sin(-\phi/3)\right], \tag{7}$$

$$B = \frac{\mathrm{i}\,k_0}{k_\perp^2} C(t_1 a\cos\phi - b\sin\phi), \tag{8}$$

and $t_1 = k_\perp\sqrt{\left(1-\dfrac{n_\mathrm{e}}{n_\mathrm{c}}\right)}$, $t_2 = \mathrm{i}\,k_\perp\sqrt{\left(\dfrac{n_\mathrm{e}}{n_\mathrm{c}}-1\right)}$.

$$a = \left[\mathrm{J}'_{1/3}(t_1\rho) - \mathrm{J}'_{-1/3}(t_1\rho)\right]\sin(\phi/3), \quad b = \left[\mathrm{J}_{1/3}(t_1\rho) - \mathrm{J}_{-1/3}(t_1\rho)\right]\cos(\phi/3),$$

here $C$ is a constant, $n_\mathrm{e}$ is the plasma density, $n_\mathrm{c}$ is the cut-off density, $\rho$ is the radius of plasma cylinder and $\mathrm{J}_{1/3}(\xi)$, $\mathrm{J}_{-1/3}(\xi)$, $\mathrm{J}'_{1/3}(t_3\rho)$, $\mathrm{J}'_{-1/3}(t_3\rho)$ are Bessel functions.

Similarly, when $n_\parallel > 1$, or $k_\parallel > k_0$,

in the inner of plasma
$$E_z = C\left[\mathrm{J}_{1/3}(t_4\rho)\sin(\phi/3) + \mathrm{J}_{-1/3}(t_4\rho)\sin(-\phi/3)\right], \tag{9}$$

in the edge of plasma
$$E_z = C\left[\mathrm{J}_{1/3}(t_3\rho)\sin(\phi/3) + \mathrm{e}^{\mathrm{i}\,\pi/3}\mathrm{J}_{-1/3}(t_3\rho)\sin(-\phi/3)\right], \tag{10}$$

$$B = \frac{\mathrm{i}\,k_0}{k_\perp^2} C(t_3 d\cos\phi - e\sin\phi), \tag{11}$$

and $t_3 = \mathrm{i}\,k_\perp\sqrt{\left(1-\dfrac{n_\mathrm{e}}{n_\mathrm{c}}\right)}$, $t_4 = -k_\perp\sqrt{\left(\dfrac{n_\mathrm{e}}{n_\mathrm{c}}-1\right)}$,

$$d = \left[\mathrm{J}'_{1/3}(t_3\rho) - \mathrm{J}'_{-1/3}(t_3\rho)\mathrm{e}^{\mathrm{i}\,\pi/3}\right]\sin(\phi/3), \quad e = \left[\mathrm{J}_{1/3}(t_3\rho) - \mathrm{J}_{-1/3}(t_3\rho)\mathrm{e}^{\mathrm{i}\,\pi/3}\right]\cos(\phi/3).$$

At the junction of vacuum area and antenna, using electric fields continuity condition leads to

$$\sigma(k_\parallel, k_y)(1 - y(k_\parallel, k_y)) = \sum_{p=1}^{MJ}\sum_{n=0}^{\infty}\sum_{m=0}^{\infty}(\alpha_{mnp} + \beta_{mnp})F_{np}(k_\parallel)G_{mp}(k_y), \tag{12}$$

$$F_{np}(k_\parallel) = -\mathrm{i}\,\frac{k_\parallel}{2\pi}\frac{1-(-1)^n\mathrm{e}^{-\mathrm{i}\,k_\parallel b}}{k_\parallel^2 - \left(\dfrac{n\pi}{b}\right)^2}\mathrm{e}^{-\mathrm{i}\,k_\parallel z_p}, \tag{13}$$

$$G_{mp}(k_y) = -\mathrm{i}\,\frac{k_y}{2\pi}\frac{1-(-1)^m\mathrm{e}^{-\mathrm{i}\,k_y a}}{k_y^2 - \left(\dfrac{m\pi}{a}\right)^2}\mathrm{e}^{-\mathrm{i}\,k_y y_p}\mathrm{e}^{-\mathrm{i}\,k_y a/2m}. \tag{14}$$

Similarly, using magnetic fields continuity condition at the junction of vacuum and plasma area leads to

$$\beta_{wvl} + \mathrm{e}^{-\mathrm{i}\,\varphi_l}\sum_{p=1}^{N}\mathrm{e}^{\mathrm{i}\,\varphi_p}\sum_{w=0}^{\infty}\sum_{v=0}^{\infty}K_{wnvm}(l,p)\beta_{wvl} = H_{wvl}, \tag{15}$$

$$K_{wnvm}(l,p) = \frac{16\pi^2\,\mathrm{i}\,\gamma_{wn}\gamma_{vm}}{ab}\iint_{-\infty}\mathrm{d}k_\parallel\mathrm{d}k_y\frac{F^*_{wl}(k_\parallel)F_{np}(k_\parallel)G^*_{vl}(k_y)G_{mp}(k_y)}{k_\perp}\frac{1+y(k_\parallel,k_y)}{1-y(k_\parallel,k_y)}, \tag{16}$$

$$H_{wvl} = \mathrm{e}^{\mathrm{i}\,\varphi_l}\alpha_{wvl} - \sum_{p=1}^{N}\mathrm{e}^{\mathrm{i}\,\varphi_p}\sum_{w=0}^{\infty}\sum_{v=0}^{\infty}K_{wnvm}(l,p)\alpha_{wvl}, \tag{17}$$

here, $F^*_{wl}(k_\parallel)$, $G^*_{vl}(k_y)$ are complex conjugate of $F_{np}(k_\parallel)$ and $G_{mp}(k_y)$. Moreover, at the junction of vacuum and plasma area, considering the impedance equality condition, we can obtain the LHW power reflection $y(k_\parallel, k_y)$ and antenna's power spectrum distribution.

## 3. Simulation results and analysis

In order to calculate the power spectrum including poloidal and toroidal coupling, we take HT-7 multi-junction (MJ) antenna as the example, which is a phase-controlled MJ coupler (3(rows)× 4(columns)×4(subwaveguides)),[5] feeding $f = 2.45$ GHz LHW to plasma. The model of LHW coupling to plasma is shown in Fig. 1. In the poloidal direction, the parameters are as follows: $d = 20.0$ mm (distance of waveguide in the poloidal direction), $a = 109.2$ mm (width of waveguide in the poloidal direction). In the toroidal direction, the parameters are as follows: $b = 10.0$ mm (width of waveguide in the toroidal direction), $c = 3.0$ mm (distance of waveguide in the toroidal direction), which has been described in Ref. [6].

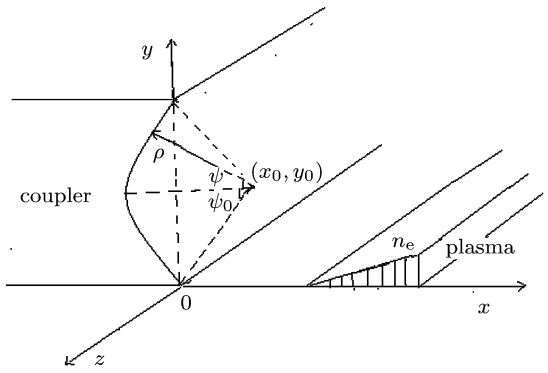



**Fig. 1.** Model of LHW coupling to plasma, assuming a plasma model consisting of a density ramp beginning at zero density at the plasma edge, with a vacuum region separating the plasma from the coupler.

### 3.1. Power spectrum

Using the above method, we estimate the power spectrum in poloidal and toroidal direction, which are displayed in Figs. 2 and 3 respectively. In order to see the effect of phase difference in the poloidal direction on the power spectrum, we calculated the poloidal spectra with the poloidal phase differences of $\Delta\psi = 0°$, $90°$, $130°$ and $180°$, which are shown in Fig. 2 and the corresponding peak values of the refractive index are outlined in Table 1. It is seen that the peak value of $n_y$ close to zero in the case of $0°$, meaning that there is no poloidal propagation in this case. With the increase of phase difference, the peak value also increases. The results are consistent with the toroidal spectra, which are shown in Fig. 3 and Table 2. A symmetric spectrum is obtained when $\Delta\psi = 180°$. The calculated result is similar to that of Berio S and Bilet Ph's in 1996.

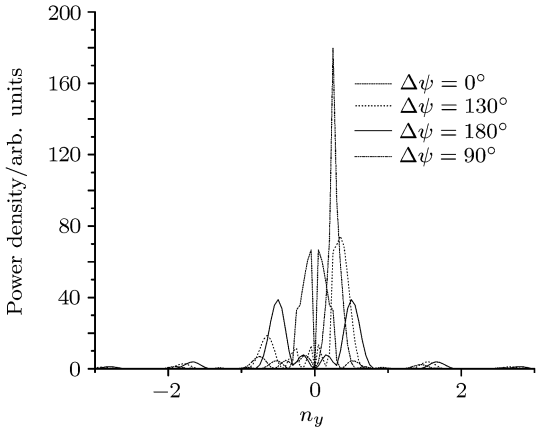



**Fig. 2.** Poloidal spectra of 3 poloidial arrays ($\Delta\psi = 0°$, $90°$, $130°$ and $180°$).

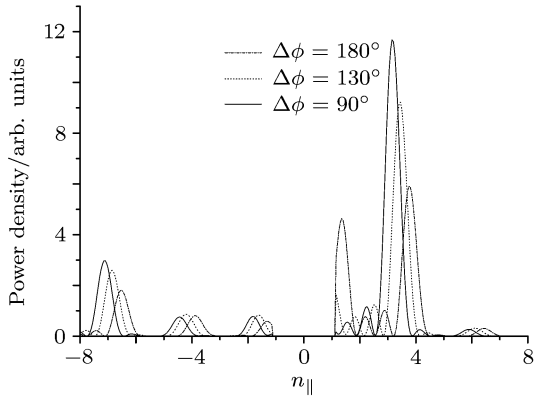



**Fig. 3.** Toroidal spectra with different phase differences ($\Delta\phi = 90°$, $130°$ and $180°$).

**Table 1.** The values of the poloidal wave vector with different phase differences.

| $\Delta\psi$ | $0°$ | $90°$ | $130°$ | $180°$ |
|---|---|---|---|---|
| $n_y$ | 0.06 | 0.25 | 0.34 | 0.51 |

**Table 2.** The values of the toroidal wave vector with different phase differences.

| $\Delta\phi$ | $90°$ | $130°$ | $180°$ |
|---|---|---|---|
| $n_\parallel$ | 3.15 | 3.42 | 3.80 |

### 3.2. Comparison of results

As mentioned in the introduction, the poloidal vector will change the injection direction, hence affect the wave propagation. In order to see the effect of the poloidal wave vector on wave propagation, power deposition and driven current, we would like to compare the results by running LHCD code[7] with different poloidal spectra ($\Delta\psi = 0°$, $90°$) in the case of $\Delta\phi = 90°$. Note that in the simulation only the power in the toroidal spectrum and the

toroidal driven current are considered. To see its effects more clearly two kinds of plasma parameters (the lower and the higher) are used in the simulation. The lower parameters are: the plasma current $I_{\rm p} = 150$ kA, magnetic field $B_{\rm t} = 1.9$ T, the central electron temperature $T_{\rm e}(0) = 0.7$ keV, the central electron density $n_{\rm e}(0) = 1.6 \times 10^{19}$ m$^{-3}$, and LHW power $P_{\rm LHW} = 350$ kW. The higher parameters are: $I_{\rm p} = 150$ kA, $B_{\rm t} = 1.9$ T, $T_{\rm e}(0) = 1.2$ keV, $n_{\rm e}(0) = 2.5 \times 10^{19}$ m$^{-3}$, and $P_{\rm LHW} = 350$ kW. The propagation results are displayed in Fig. 4. It is seen that ray tracings are different with the different phase differences in the two kinds of plasma parameters, due to the different injection direction. Due to such difference of propagation, there is some difference in the power deposition and driven current.

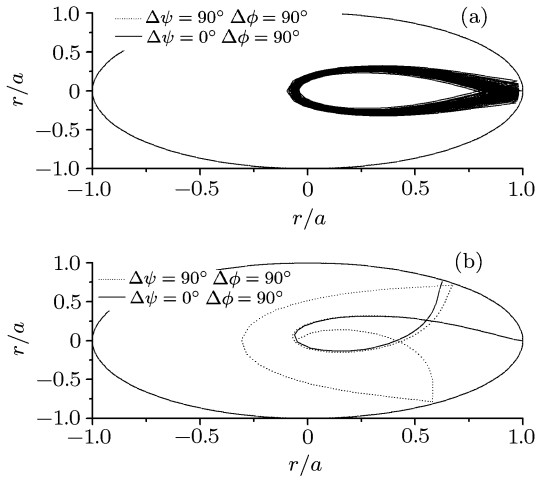



**Fig. 4.** LHW ray traces with $\Delta\psi = 0°$ and $\Delta\psi = 90°$ ($\Delta\phi = 90°$): (a) in the lower plasma parameter; (b) in the higher plasma parameter.

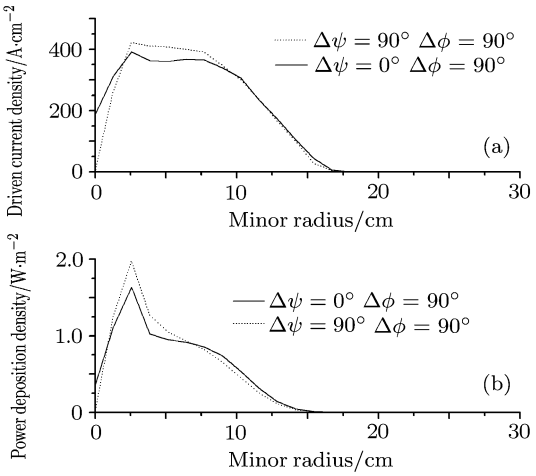



**Fig. 5.** Driven current profile: (a) LHW power deposition; (b) with $\Delta\psi = 0°$, 90° and $\Delta\phi = 90°$ in the lower plasma parameter.

As seen from Figs. 5 and 6, simulations show that there is little effect of the poloidal wave vector on profiles of power deposition and driven current in the low parameter case, whereas profiles of power deposition and driven current obviously move inward in the high parameters, suggesting that the poloidal wave vector also has a different influence on power deposition and driven current in the different plasma parameters. Compared to the higher parameters, in the low parameter plasma, the LHW power is absorbed after multi-pass propagation (see Fig. 4), the power deposition is mainly located in the core region (see Fig. 5). Possibly due to the multi-pass absorption, the effect on power deposition and driven current in the higher parameter plasma is larger than that in the lower parameter case.

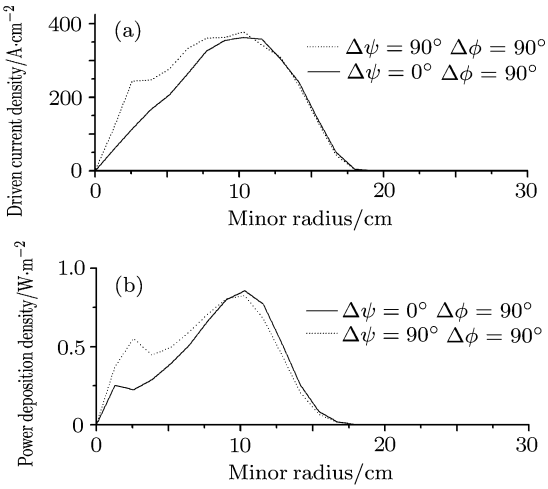



**Fig. 6.** Driven current profile: (a) LHW power deposition; (b) with $\Delta\psi = 0°$, 90° and $\Delta\phi = 90°$ in the higher plasma parameter.

# 4. Discussion

Present results show that by considering the poloidal phase difference, the poloidal spectrum is different, leading to a different injection direction of the wave beam. As a result, it affects the wave propagation. When the poloidal phase difference is $\Delta\psi = 0°$, the value of the poloidal wave vector closes to zero, implying that the effect of the poloidal vector can be neglected in this case. Simulation shows that the poloidal wave vector really has an effect on the power deposition and driven current, suggesting that it is possible to control current profile by adjusting the poloidal phase difference purposely, especially when the range of toroidal spectrum which can be adjusted is small in order to pursue high directivity and high current driven efficiency for the MJ antenna.

Of course, in the real plasma, the phase difference in the poloidal direction due to the mismatch between the plasma and LHW antenna is small, so its effect on propagation and power deposition should be much smaller than that in the case of $\Delta\psi = 90^\circ$.

## 5. Conclusion

By the way of numerical simulation, the power spectrum considering coupling between the waveguides in both poloidal and toroidal directions are estimated, nearly similar to the results of Berio S and Bilet Ph's in 1996. Further calculation shows that the dependence of poloidal spectrum on poloidal phase difference is similar to the toroidal case, peak value increases with the increasing phase difference. By changing the poloidal phase difference, the propagation of LHW in plasma is different due to the different injection direction, leading to a different power deposition and a different driven current profile. The effect of the poloidal wave vector on power deposition and driven current profile depends on plasma parameters. Results show that the poloidal wave vector also has an effect on power deposition and driven current, especially in the case of high parameter plasma, and it seems possible to control the current profile with the help of adjusting the poloidal phase difference.

## References


[1] Brambilla M 1976 *Nucl. Fusion* **16** 47

[2] Berio S and Bilet Ph 1996 *23rd EPS on Controlled Fusion and Plasma Physics* **e017** 887

[3] Brambilla M 1978 *Nucl. Fusion* **18** 493

[4] Ma Z F, Li D F and Chen J 1982 *Acta Phys. Sin.* **31** 159 (in Chinese)

[5] Wang M, Liu Y X, Shan J F, Liu F K, Xu H D and Ding B J 2003 *Nucl. Fusion Plasma Phys.* **23** 55 (in Chinese)

[6] Ding B J, Shan J F, Liu F K, Fang Y D, Wei W, Wu Z W, Chen Z Y, Xu H D, Wang W, Jiang M, Zhang G R, Huang F, Zhao Y P, Kuang G L and HT-7 Team 2006 *Chin. Phys.* **15** 2989

[7] Ding B J, Kuang G L, Liu Y X, Shen W C, Yu J W and Shi Y J 2002 *Acta Phys. Sin.* **51** 2556 (in Chinese)